

The development of a nonstationary separation and coherent structures in a two-dimensional viscous incompressible flow around a body

M.N. ZAKHARENKO (MOSCOW)

*Dedicated to the memory of Vladimir M. Galkin
killed in an aircraft crash in September 1994*

TWO-DIMENSIONAL VISCOUS incompressible flows around a circular cylinder and a 12% Zhukovsky airfoil are considered. Numerous examples of complex separated flows around these bodies with coherent structures and detached separation generation, as well as examples of flow stabilization and separation destruction are obtained. Numerical experiment technology based on parametrization of the far-field boundary conditions and effect of sequential exclusion of the scheme parameters and problem statement disadvantages is proposed.

1. Problem statement

THE STATEMENT of the problem and solution procedure are detailed in [1, 2]. Two-dimensional $N - S$ equations are written in terms of the stream function Ψ and vorticity Ω , which are defined by relations $u = \partial\Psi/\partial y$, $v = -\partial\Psi/\partial x$, $\Omega = \partial u/\partial y - \partial v/\partial x$:

$$(1.1) \quad \Delta\Psi = H^2\Omega,$$

$$(1.2) \quad H^2 d\Omega/dt = \text{Re}^{-1} \Delta\Omega,$$

where H^2 is the Jacobian of transformation of Cartesian coordinates x, y to curvilinear orthogonal coordinates ξ, η . A grid of "O"-type obtained by a conformal mapping of an airfoil onto a circle is used. $\text{Re} = U_\infty b/\nu$ is the Reynolds number, where U_∞ is a free stream velocity, b is a characteristic length, ν is coefficient of kinematic viscosity. Dimensionless time t is defined by the relation $t_{\text{phys}} = tb/U_\infty$, where b is either the chord of airfoil or $b = R$ is radius of the cylinder.

Boundary condition. On a solid body surface S the following no-slip conditions are defined:

$$v_\xi = -H^{-1} \partial\Psi/\partial\eta \Big|_S = \varphi(\eta), \quad v_\eta = H^{-1} \partial\Psi/\partial\xi \Big|_S = f(\eta).$$

The condition $\partial\Psi/\partial\xi \Big|_S = Hf(\eta)$ is transformed into a boundary condition for a vorticity Ω_S [1, 3] by using a two-parameter approximating formula; this permits

us to eliminate the approximation effect on the solution accuracy and to maximize the iterative solution process rate by employing the procedure described in [1].

Over the far boundary S_∞ (being about 10 chords away from the body), the following boundary conditions are specified:

$$(1.3) \quad \partial\Omega/\partial\xi = 0,$$

$$(1.4) \quad \partial\Psi/\partial\xi = v_\infty \left(\frac{\partial x}{\partial\xi} \sin\alpha - \frac{\partial y}{\partial\xi} \cos\alpha \right) - \frac{v_\infty}{R_\infty} [D_x \sin(\eta - \alpha) + D_y \cos(\eta - \alpha)] - \Gamma/2\pi,$$

where D_x , D_y and Γ are parameters.

The flow starts from the state when the body and fluid are at rest.

2. Method of solution

A solution of decoupled equations of the system is used. Equation (1.1) is solved directly by expansion into a Fourier series in terms of the cyclic coordinate η .

Equation (1.2) is solved by the ADI method. Central differences for second derivatives and one-sided upwind differences for nonlinear terms in (1.2) are used.

At each time step an iterative process is employed. A zonal approach used in [4] is applied.

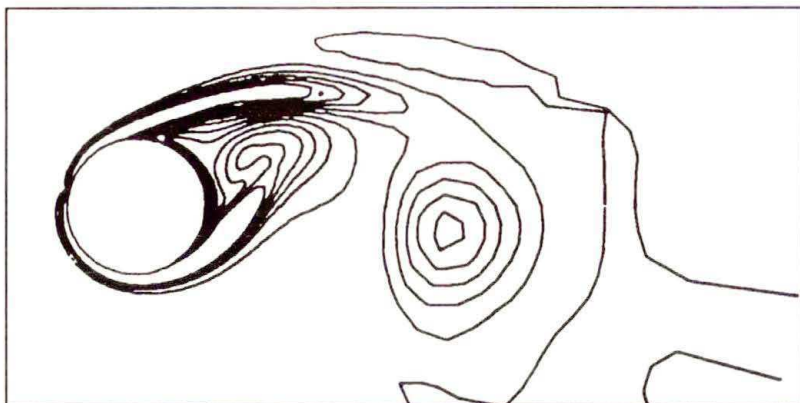
3. Flow past a circular cylinder

Two problems are considered.

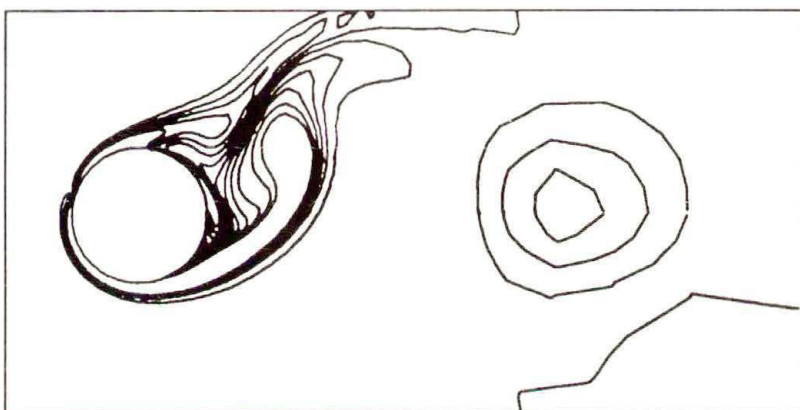
3.1.

Uniform flow around a circular cylinder in a viscous incompressible fluid that is preliminarily spun can serve as an interesting example. An initially steady flow around a cylinder rotating at a constant angular velocity W in a uniform viscous flow has been obtained by calculation for $\text{Re} = U_\infty R/\nu = 200$ (R denotes the radius of the cylinder) and Rossby number $\text{Ro} = WR/U_\infty = 2$. In this case the boundary conditions on S_∞ include the circulation term, as in [5, 6, 7]. When the flow becomes steady, the cylinder is suddenly stopped. If we apply in this case the widely used argument that the velocity over S_∞ will change when cylinder-induced vortical disturbances carried by the flow reach this boundary, we conclude that after a long time (comparable with the distance between S and S_∞), the presence of the vortex term in the asymptotic on S_∞ will be retained.

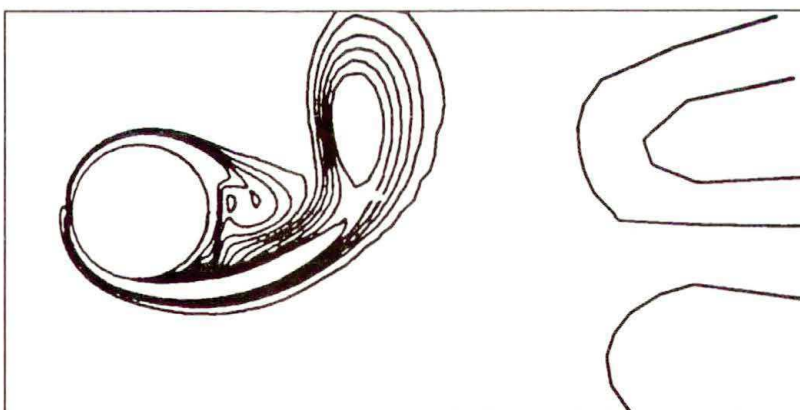
The equi-vorticity lines are shown in Fig. 1 for the solution to $N - S$ equations when the problem statement includes (i) no-slip boundary condition over



a) $t = 16$



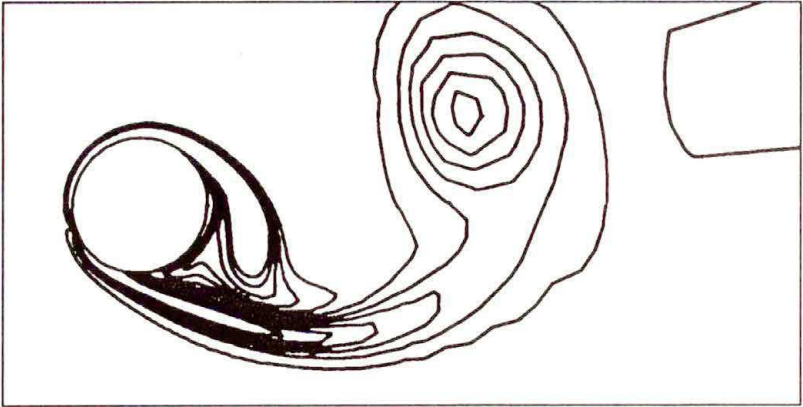
b) $t = 18$



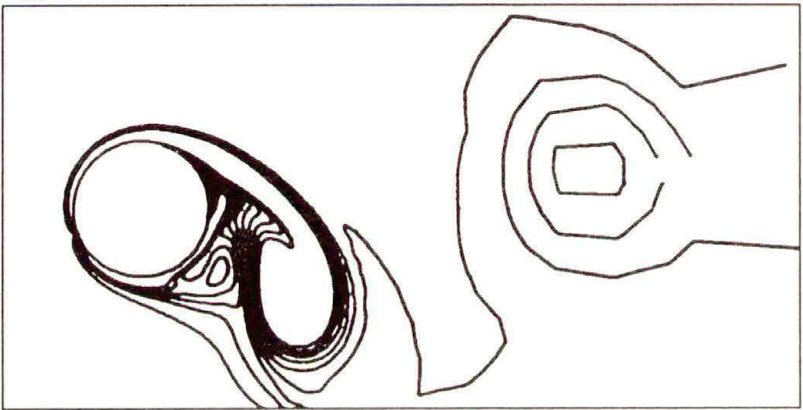
c) $t = 20$

[FIG. 1 a, b, c]

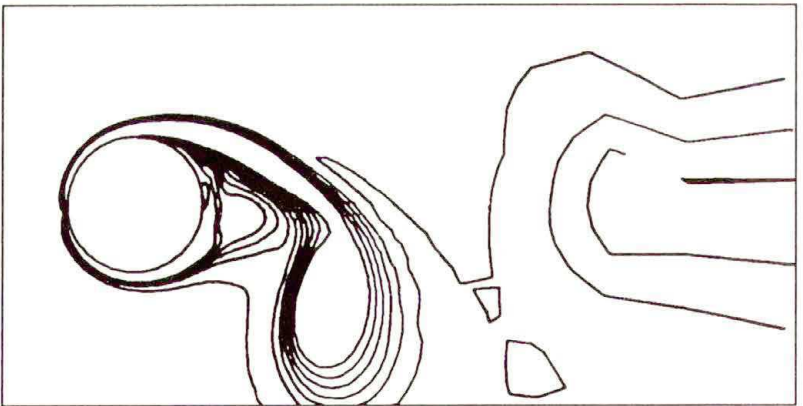
[397]



d) $t = 22$



e) $t = 24$



f) $t = 25$

[FIG. 1 d, e, f]

FIG. 1.

S for immovable cylinder, and (ii) uniform flow with circulation term over S_∞ . Reversed Kármán street is observed: a vortex A , leaving the upper side of the cylinder, gets down and is then found under the vortex B which has departed from the lower side of the cylinder; and simultaneously, all vortex street is carried downwards due to the flow spinning effect (or upwards, if the flow has been spun in the opposite direction). The first vortices of Golubev street [8] are obtained. It follows that a thrust is generated.

The computation domain size is limited to 20 radii of the cylinder. Therefore the vortex street development is computed over a time interval $\Delta t = 15$. In this case it is clear that changes over S_∞ will occur earlier than the wake will reach it. It is obvious that, after the initial vortex street reversal, some time is necessary for the Kármán street to be restored.

To study this phenomenon, the computation domain size should be expanded and the problem of proper boundary conditions for S_∞ should be solved. In view of technical problems, a more powerful computer than MICROVAX-2 is desirable.

3.2.

Detached separation in flow around a circular cylinder which performs angular oscillations about its axis in a free stream has been studied previously in [4]. The law of oscillations is as follows:

$$W = \frac{1}{2} A \sin(\omega(t - t_0)), \quad \omega = 2\pi K, \quad K = R/U_\infty T.$$

Figure 2 a presents the equi-vorticity lines at $Re = 35$. The oscillation amplitude $A = 45^\circ$, reduced frequency $K = R/U_\infty T = 3$ (T is an oscillation period); Fig. 2 b presents the streamlines. One can see a symmetrical separation region that is separated from the cylinder by the circular layer in which the flow is essentially unsteady.

At Reynolds numbers as high as 200, the flow topology presented in Fig. 2 is conserved [4]. Effects of scheme parameters were studied by diminishing the mesh steps in both space and time.

A further study of the problem is concerned with the opportunity of flow stabilization of the previously developed separated flow. The unsteady flow with a Kármán street (Reynolds number $Re = 200$) past a circular cylinder was taken as an initial state. Attempts to attain flow stabilization were made with the help of angular oscillations of the cylinder about its axis with the reduced frequency $k = 3$ at $A = 45^\circ$. Survey of the equi-vorticity lines in Fig. 3 raises the question about an intermediate separation, when detached separation with asymmetrical flow pattern alternates with the attached (conventional) separation. The vortex is detached from the cylinder surface by a liquid layer and the inflowing liquid particles do not reach the cylinder [4]. To compare, one can refer to Fig. 1 drawn

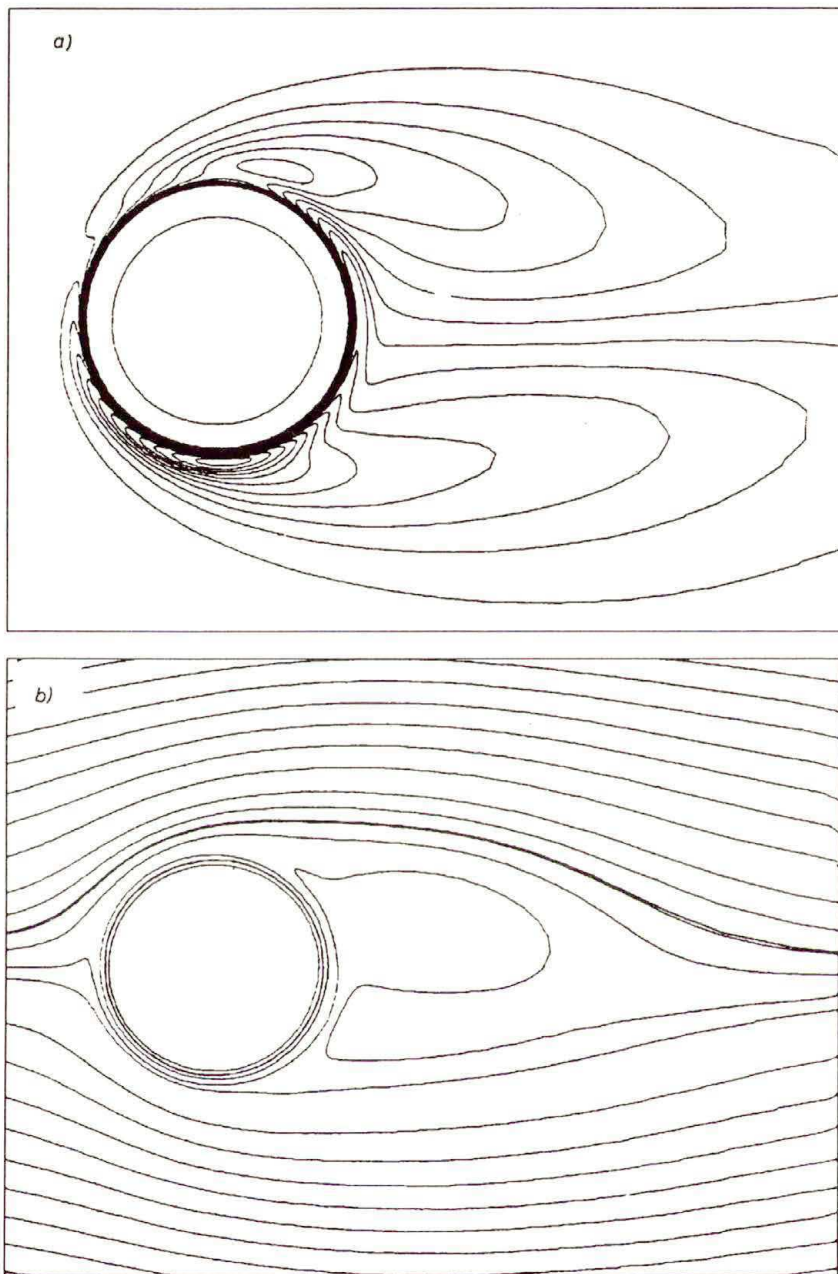
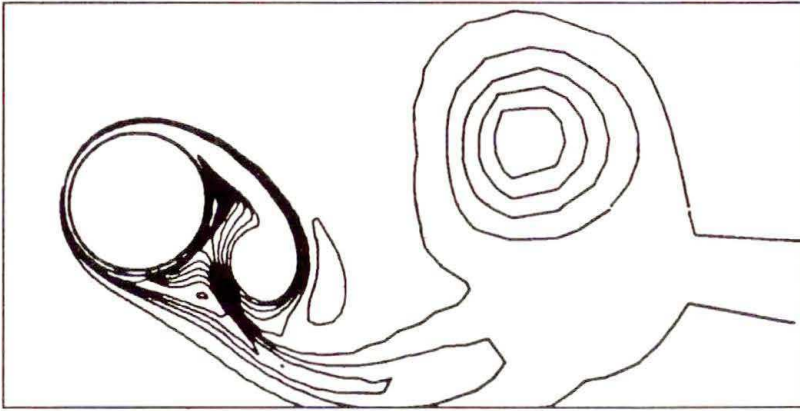
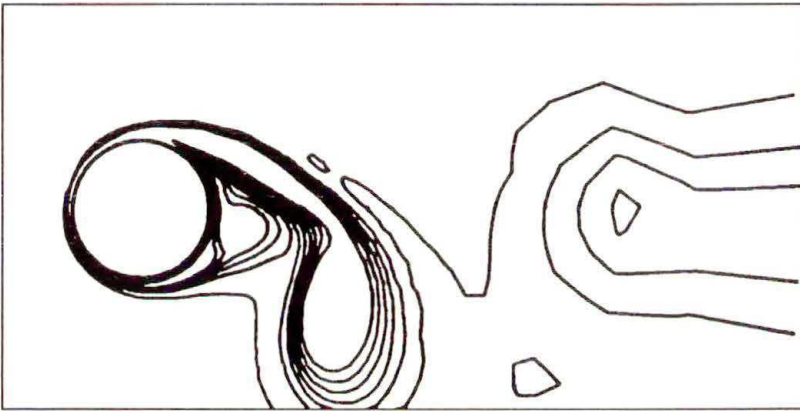


FIG. 2.

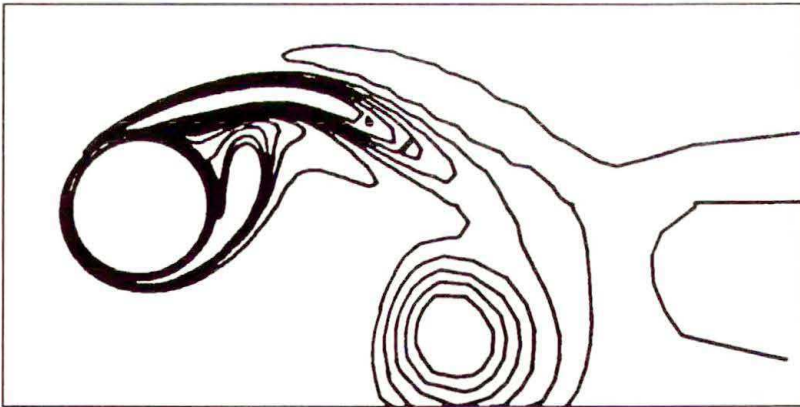
[400]



a) $t = 23$



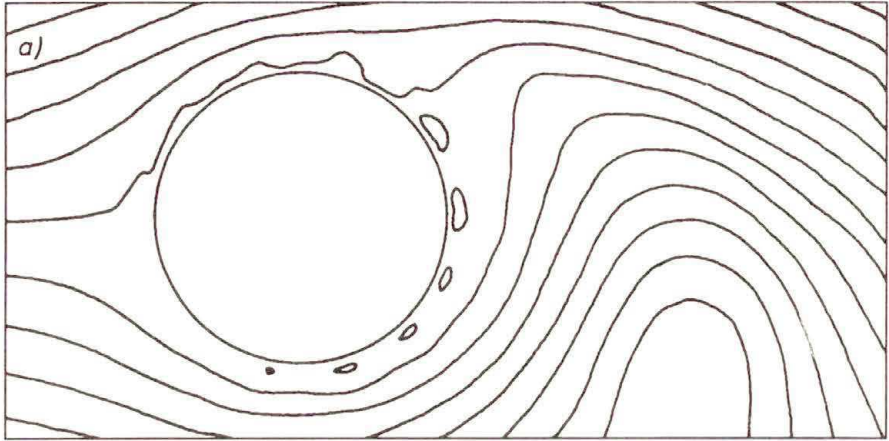
b) $t = 25$



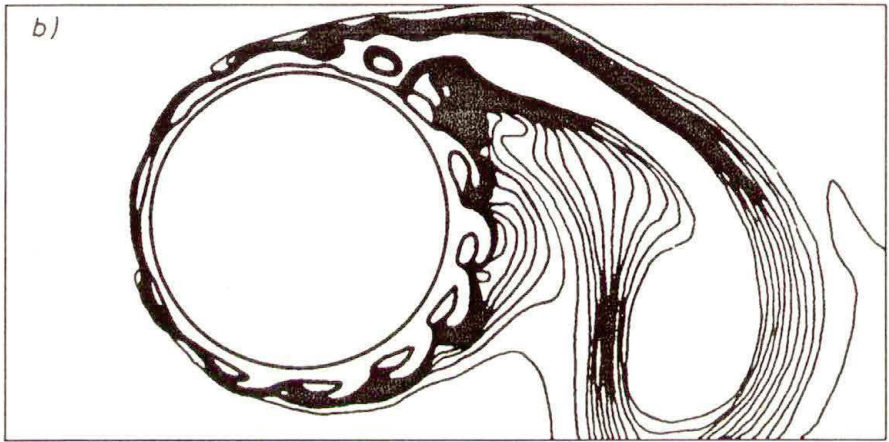
c) $t = 27$

FIG. 3.

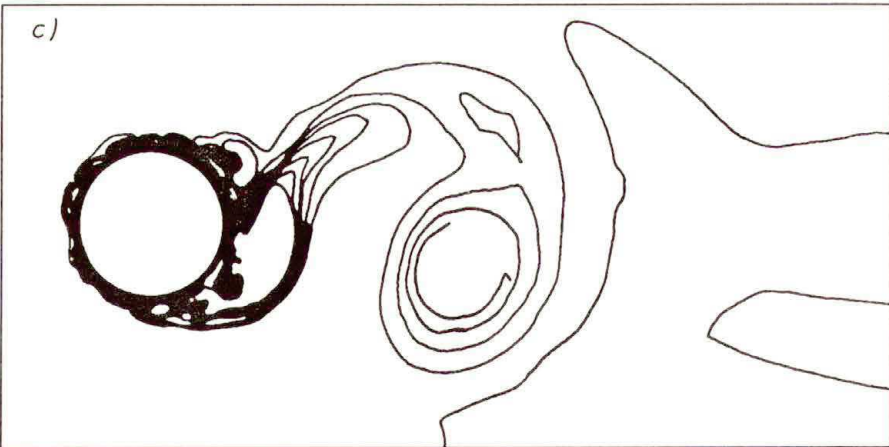
[401]



$t = 23$



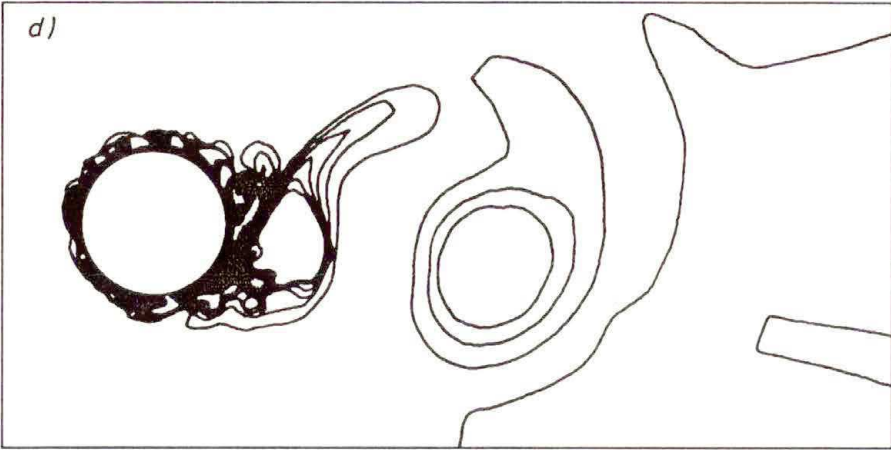
$t = 23$



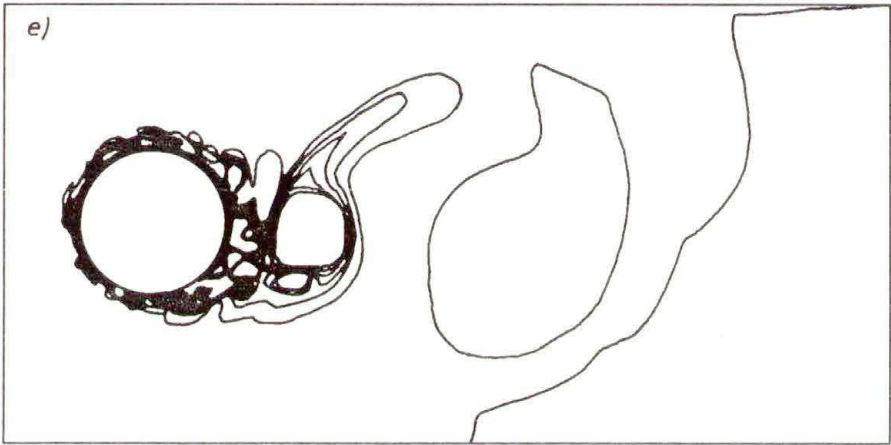
$t = 26.025$

[FIG. 4 a, b, c]

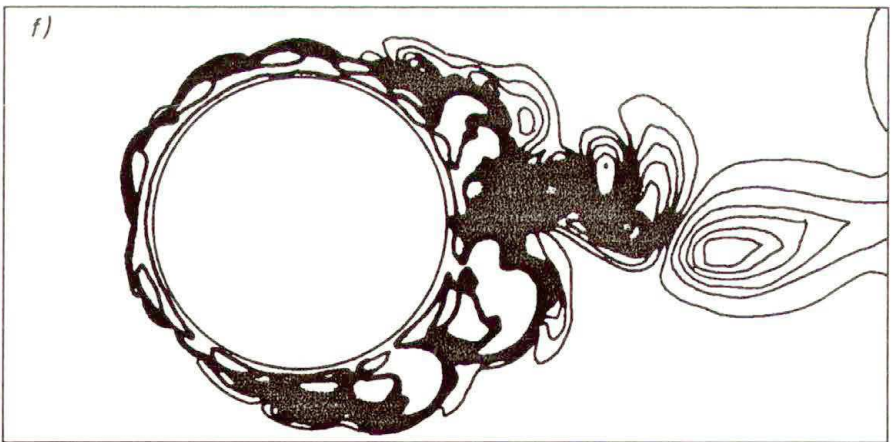
[402]



$t = 26.55$



$t = 26.9$



$t = 30.225$

FIG. 4.

[403]

for a cylinder at the same Reynolds number, but without angular oscillations. No differences in generation and motion of vortices are seen. Differences in geometry of vortices and hence in their intensity are also not observed.

However, changing the scheme parameters results in an unexpected new type of flow presented in Fig. 4. In this case the calculations are stable and, with parameters of the finite-difference scheme being fixed, the results converge precisely to the revealed solution. Different solutions at different parameters of a finite-difference scheme means the lack of convergence in a strong mathematical sense. So some new aspects of the computational fluid dynamics theory must be developed.

Small vortices generation presented in Fig. 4 reduces the intensity of primarily separated vortices, which move away from the cylinder, and even eliminates the generation of large vortices that are known as a vortex street of the Kármán street type. A completely different topology is realized (Fig. 4).

Note that the time interval from $t = 23.0$ to $t = 30.225$ when such changes have taken place, is quite short and comparable with the specific period of vortex generation in the Kármán street.

At $Re = 35$ small vortices are not generated, with any finite-difference scheme parameters. A considerable growth of errors in the region of the reversal wake flow is observed at a time step greater than a certain value. In such a way, at this Reynolds number the solution converges only to the unique flow pattern, which is identified as the detached separation, see Fig. 2.

The examples presented have raised the problem of estimation of adequacy of a numerical solution to physical reality.

4. Numerical experiment for a flow past an airfoil

Numerical experiment technique was designed for the problem of flow past an airfoil. Primary effect of specifying the circulation term for a velocity over S_∞ on the solution was studied. Flow past the 12% Zhukovsky airfoil with a finite trailing edge angle at $Re = 10^4$ and angle of attack $\alpha = 5^\circ$ was estimated. For the boundary condition (1.4) $D_x = D_y = 0$ was specified. There exists the range of values $\Gamma = (0 : -0.21)$ where the condition of pressure uniqueness over the trailing edge is satisfied [9, 10]. The pressure coefficient $C_p = (p - p_\infty) / \frac{1}{2} \rho U_\infty^2$ is presented in Fig. 5, where a) $\Gamma = 0$; b) $\Gamma = -0.21$; c) $\Gamma = -0.40$. The vortex within the domain limited by S_∞ is placed rather arbitrarily. For example, when the centre of the vortex with intensity $\Gamma = -0.21$ lies on the positive Ox axis downstream the airfoil at $X_\gamma = 0.5$ or $X_\gamma = 2$, we obtain the coefficient C_p presented in Fig. 5 d or 5 e, respectively. Pressure coefficient C_p in both cases is the same and close to that occurring in the case with $X_\gamma = 0$ (Fig. 5 b).

When an asymptote of far field flow with two vortices is specified over S_∞ , we conclude the following: if the second vortex is outside the domain bounded

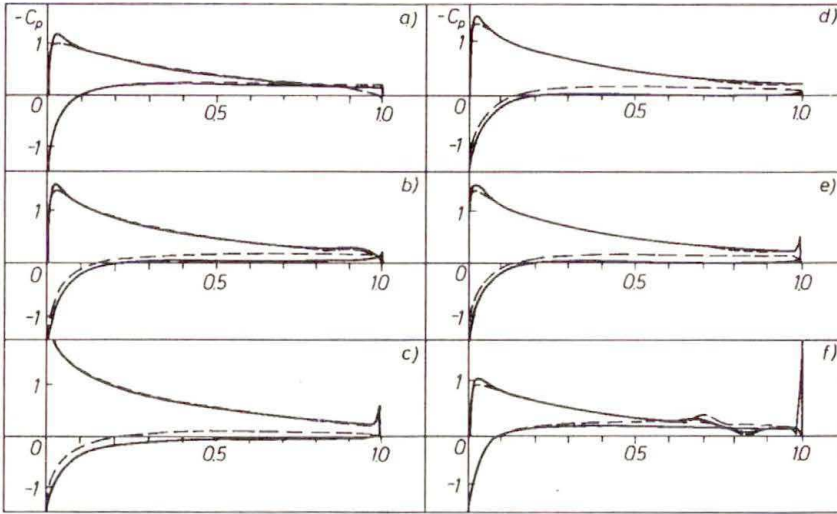


FIG. 5.

by S_∞ , then it insignificantly affects the integral characteristics and C_p (Fig. 5 f, $X_\gamma = 12$, $\Gamma = -0.21$). In this case the first vortex can be located inside the computational region (bounded by S_∞) arbitrarily, retaining the integral characteristics unchanged. Such a dependence of Γ on S_∞ and C_p emphasizes the connection of this asymptotics with the lifting capability of the airfoil and makes it very suitable for modelling these phenomena.

The dipole term effect was studied. For example, Fig. 6 presents the streamlines and the equi-vorticity lines (Fig. 6 e) in the vicinity of the 1/4 chord of the 12% Zhukovsky airfoil; Reynolds number $Re = 10^4$, angle of attack $\alpha = 7.25^\circ$. Parameters in (1.4) are as follows: $D_x = D_y = \Gamma = 0$ (Fig. 6 a-f) and $D_x = -4$, $D_y = 4$, $\Gamma = -0.20$ (Fig. 6 g-l). Development of coherent vortex structures in the vicinity of the trailing edge was obtained. This study is discussed in detail in [2].

The next step of the investigation is to study the flow with an increasing Reynolds number. Figure 7 presents the streamlines (7 a-7 f) and equi-vorticity lines (7 g-7 l) for the 12% Zhukovsky airfoil at $\alpha = 5^\circ$, $D_x = D_y = 0$ and $\Gamma = -0.21$, when the Reynolds numbers are the following: a), g) $Re = 1.5 \times 10^4$; b), h) $Re = 2 \times 10^4$; c) i) $Re = 2.5 \times 10^4$; d), j) $Re = 3 \times 10^4$; e), k) $Re = 3.5 \times 10^4$; f), l) $Re = 3.75 \times 10^4$.

Considerable development of separation over the leeward side of the airfoil is observed. Reynolds number of 37500 is the highest value at which the computation convergence in the framework of laminar flow is obtained (at $\alpha = 5^\circ$). In this experiment the computations are performed with successively increasing Re and the flow for previous Re is the initial condition for computations of flow at a next Re . The fact that distributions C_p over S (Fig. 8 a for $Re = 15000$), obtained by integrating (along the different paths but with the same method of integration)

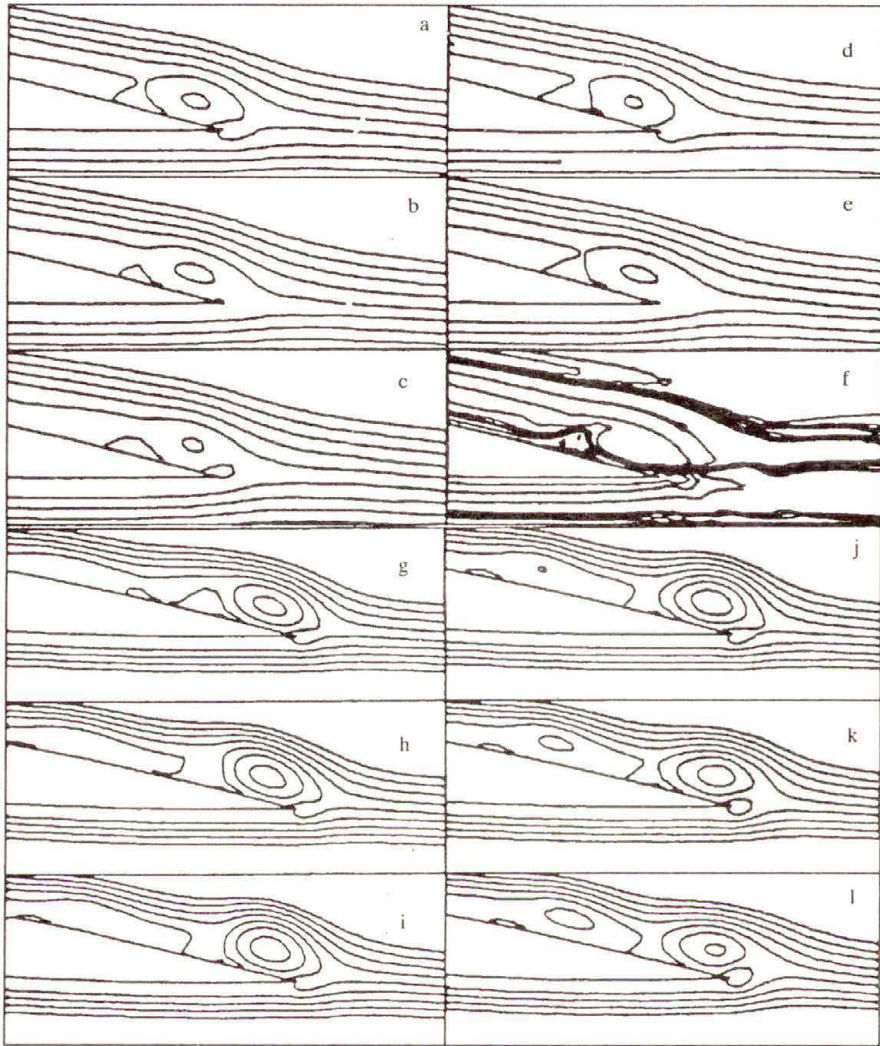


FIG. 6.

the equation of motion, do not coincide, indicates that the solution is not quite correct [11]. The study in [12] for a circular cylinder rotating in viscous flow shows that asymptotic condition for far field flow may be properly stated so as to eliminate the pressure nonuniqueness. This is one of the goals of our study of the viscous flow around a body with boundary conditions (1.3) and (1.4), where the number of terms in the asymptotic expansion may be increased.

The effect of scheme factors and parameters of the mathematical model on the problem solution is studied. It has been found that, within the investigated angles-of-attack and Reynolds numbers ranges, the flow turbulization cannot yet

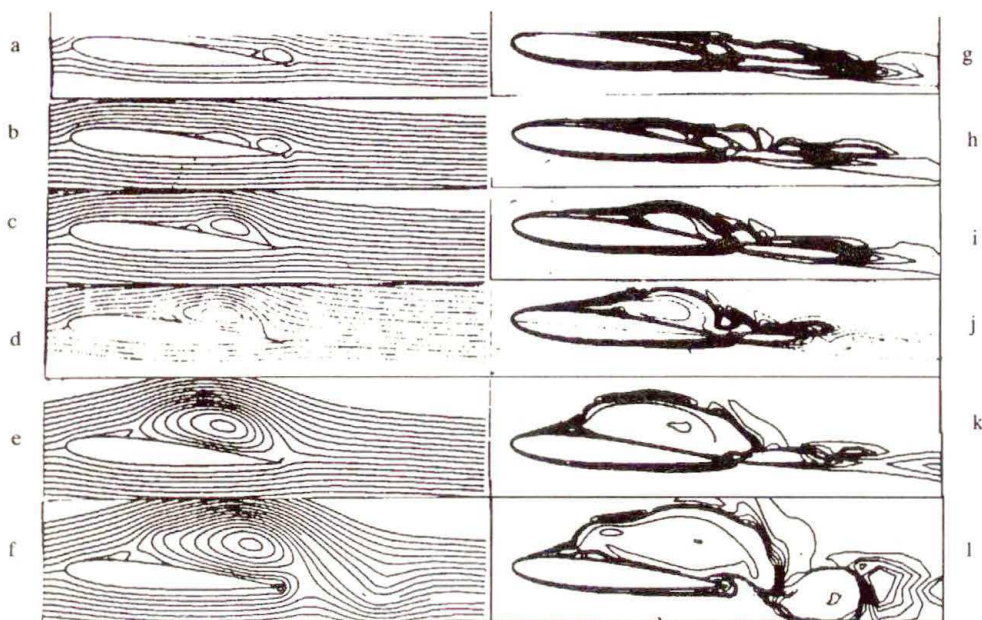


FIG. 7.

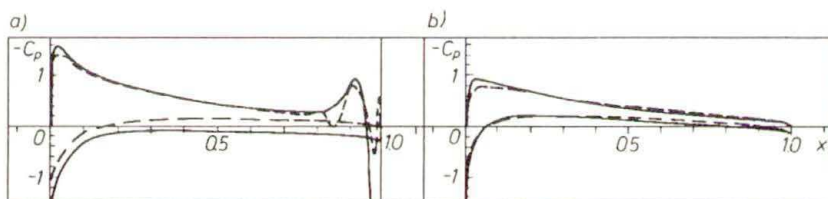


FIG. 8.

reduce the separation region, presented in Fig. 7. The Baldwin-Lomax model was used.

The search of explanations of the causes of the presented topology of flow around an airfoil results in construction of a flow model including a laminar wake [13]. In this case the theory suggests the solution in which the flow in the wake conserves (and convects) momentum losses of two types. The first one defines the drag acting on an airfoil due to viscous friction. The second one corresponds to lift variation. Those losses must occur within the near-wall layer and then be convected by the wake. In the framework of this theory, construction of distributed sources and sinks is necessary.

We will synthesize the above-mentioned theory [13] with the Lighthill construction [14], where the near-wall layer momentum losses are simulated by distributed sources and sinks with their extension into the wake. The latter combines the suggestion of [13] and the model of [14].

However, practical application of the part of this theory which deals with specification of distributed wake singularities is a difficult problem. It has been found that application of this model doesn't resolve yet all the difficulties which we have in numerical solution for the flow presented in Fig. 7. Thus, generation of a developed separated flow is connected with construction of a general asymptotic behaviour of the solution for flow around an airfoil.

A detailed study by including additional sources, dipoles and vortex terms in the asymptotic expansion for velocity over S_∞ was conducted. It is obtained that at least one of possible representations includes the additional asymptotics of two vortices with opposite signs of circulation and their centres are located inside the airfoil.

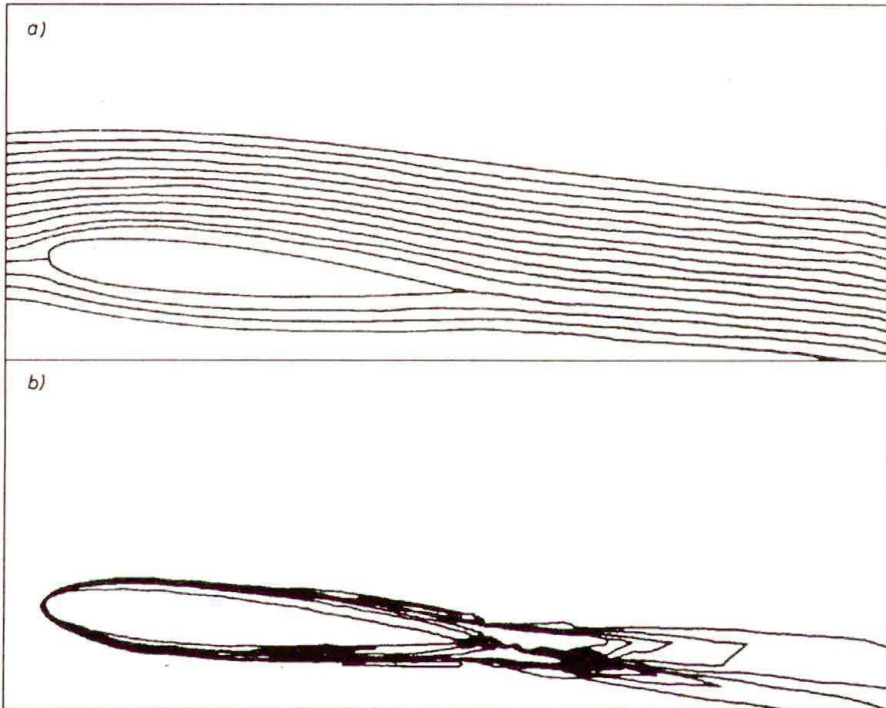


FIG. 9.

Figure 9 a, b present the topology for $Re = 1.5 \times 10^4$, $\alpha = 5^\circ$, and Fig. 8 b, the pressure distribution when the mentioned singularities are added to the initial state shown in Fig. 7 a, g. As we see, the flow obtained is similar to that studied before at $Re = 10^4$ and $\alpha = 5^\circ$ and is in agreement with our knowledge of the full-scale experiment. Note that the separation region disappears, what is especially clear in comparison with flow in Fig. 7. The agreement between C_p and C_p^0 obtained by different ways of integration [11] indicates mathematical accuracy of the solution obtained.

After the same construction, the elimination of massive separation in the flow at $Re = 3.5 \times 10^4$ is obtained too. It should be noted that the flow topology singularities that were presented in Fig. 7, are still of interest to investigators because similar vortex structures are realized obviously at high angles of attack.

At last, Fig. 10 shows a distribution of circulation γ along a coordinate line $\xi = \text{const}$ as a function of the coordinate x at which this line intersects the positive Ox axis; these data indicate that, in accordance with the model of [13], solutions can be realized when value of γ is bounded by Γ given at S_∞ from below, see Fig. 10 a ($\alpha = 5^\circ$, $Re = 1.5 \times 10^4$, $\Gamma = -0.21$, $D_x = D_y = 0$) and flows where $|\gamma| < \Gamma$ (at the same Re , D_x , D_y , but the above mentioned two vortices with opposite signs of circulation are included in (1.4)). The latter means that in the airfoil wall region there occur momentum losses resulting in a decrease of C_y in comparison with that C_y defined by Γ in the framework of potential flow theory for an ideal fluid.

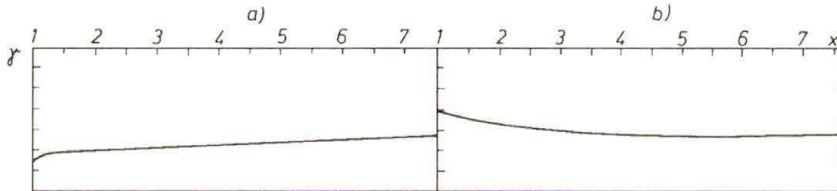


FIG. 10.

It can be noted briefly that inclusion of additional vortices into the asymptotic for S_∞ affects significantly the aerodynamic moment that is induced by the potential part of the solution. This follows from the Chaplygin–Blasius theorem for an ideal fluid. The results obtained for an ideal fluid are not related directly to viscous flows, but mechanical meaning of inclusion of the mentioned singularities – to change the aerodynamic moment – is certainly the same.

The examples presented have shown that the application of the technology of the numerical experiment allows us not only to reveal disadvantages of the problem statement but also to eliminate the difficulties. The results concerning the flow past the circular cylinder present new problems that couldn't be studied earlier in the framework of numerical experiments.

References

1. M.N. ZAKHARENKO, *On the approximation of the boundary condition for vorticity* [in Russian], [in:] Sb. Čisl. Metody Mehaniki Spl. Sredy, 13, 2, 61–81, Novosibirsk 1982.
2. M.N. ZAKHARENKO, *Analysis of detached flow behind a profile* [in Russian], Preprint CAGI, 4, 1990.
3. M.N. ZAKHARENKO, *Approximation of the boundary condition for vorticity at a solid body surface in the analysis of the Navier–Stokes equation* [in Russian], [in:] Sb. Čisl. Metody Mehaniki Spl. Sredy, 11, 7, 56–74, Novosibirsk 1980.
4. M.N. ZAKHARENKO, *Solution of nonstationary viscous flow about a cylinder performing torsional vibrations in a uniform flow*, Izv. AN SSSR, MŽG, 5, 32–38, 1989.

5. D.B. INGHAM, *Steady flow past a rotating cylinder*, *Comp. and Fluids*, **11**, 4, pp. 351–366, 1983.
6. K.V. NIKOLAEV, *Separation of the boundary layer at the surface of a rotating cylinder subject to incompressible flow* [in Russian], *Učenyje Zapiski CAGI*, **13**, 6, 32–39, 1982.
7. V.V. NEGODA, V.V. SYČEV, *On the boundary layer at a rotating cylinder* [in Russian], *Izvestija AN SSSR MŽG*, 5, 36–45, 1987.
8. V.V. GOLUBEV, *Treatise on aerodynamics*, M.-L., Gostehizdat, p. 979, 1957.
9. M.N. ZAKHARENKOV, *Far-field boundary conditions for a viscous incompressible flow past a profile*, *Matem. Modelirovanie*, 2, 3–18, 1990.
10. M.N. ZAKHARENKOV, *Unsteady incompressible viscous flow past an airfoil*, *Arch. Mech.*, **42**, 4-5, 609–615, 1990.
11. M.N. ZAKHARENKOV, *Singularities of finite-difference scheme for two-dimensional Navier–Stokes equations solution connected with the boundary condition statement on a solid surface* [in Russian], *Žurn. Vyč. Mat i Mat. Fiz.*, **30**, 8, 1224–1236, 1990.
12. H.M. BADR and S.C.R. DENNIS, *Time-dependent viscous flow past an impulsively started rotating and translating circular cylinder*, *J. Fluid Mech.*, 158, 447–488, 1985.
13. M.N. ZAKHARENKOV, *Far-field asymptotics at a viscous incompressible flow past a profile* [in Russian], [in:] *Sb. Trudy II otraslevoj Konf. po Aerodinamike Letatel'nych Apparatov, Žukovskij-Volodorskoje*, 1991.
14. M.J. LIGHTHILL, *On displacement thickness*, *J. Fluid Mech.*, pp. 383–392, 1959.

CENTRAL AERO-HYDRODYNAMIC INSTITUTE, MOSCOW, RUSSIA.

Received July 24, 1995.